



# A Novel Electrochemical Sensor Based on MnO<sub>2</sub>/Sepiolite Nanocomposite for the Detection of Hydrogen Peroxide in Human Serum Samples

AbduRahman Hosseinifar<sup>1</sup>, Masoud Ghanei-Motlagh<sup>2,\*</sup> and Maryam Fayazi<sup>3</sup>

<sup>1</sup>Transport Phenomena & Nanotechnology (TPNT) Lab., School of Chemical Engineering, College of Engineering, University of Tehran, 111554563, Tehran, Iran

<sup>2</sup>Part Nanofanavar Kavian (PNK) Company, Environmental Research Group, Kerman, Iran

<sup>3</sup>Department of Environment, Institute of Science and High Technology and Environmental Sciences, Graduate University of Advanced Technology, Kerman, Iran

\*Corresponding author: Part Nanofanavar Kavian (PNK) Company, Environmental Research Group, Kerman, Iran. Email: [m.ghaneimotlagh@yahoo.com](mailto:m.ghaneimotlagh@yahoo.com)

Received 2021 August 28; Revised 2021 October 03; Accepted 2021 October 11.

## Abstract

**Background:** The reliable and easy-to-operate detection of hydrogen peroxide (H<sub>2</sub>O<sub>2</sub>) has attracted extensive attention in the fields of biomedicine, food security, and environmental analysis.

**Objectives:** In this work, a novel electrochemical method was proposed for H<sub>2</sub>O<sub>2</sub> monitoring using a carbon paste electrode (CPE) modified with MnO<sub>2</sub>/sepiolite nanocomposite.

**Methods:** MnO<sub>2</sub>/sepiolite material was characterized by transmission electron microscopy (TEM), energy-dispersive X-ray spectroscopy (EDS), and X-ray diffraction (XRD) technique. The modified CPE was employed for the amperometric monitoring of H<sub>2</sub>O<sub>2</sub> in human serum samples.

**Results:** Electrochemical data showed that the MnO<sub>2</sub>/sepiolite-CPE displays a high peak current towards H<sub>2</sub>O<sub>2</sub> oxidation. A linear range from 5 to 700 μM and a low detection limit of 0.8 μM for H<sub>2</sub>O<sub>2</sub> were obtained with the proposed sensor. Besides, the electrode depicted excellent reproducibility and anti-interferant ability, promising the applicability of this electrochemical method in practical analyses.

**Conclusions:** This work introduced a new and effective enzyme-less H<sub>2</sub>O<sub>2</sub> sensor based on the MnO<sub>2</sub>/sepiolite nanocomposite modified CPE. The suggested sensor showed good sensitivity for the rapid detection of H<sub>2</sub>O<sub>2</sub> in a wide linear range with a low detection limit and satisfactory reproducibility, which made it practical for the analysis of hydrogen H<sub>2</sub>O<sub>2</sub> in real samples.

**Keywords:** Nanocomposite, Hydrogen peroxide, Sensor, Human Serum

## 1. Background

H<sub>2</sub>O<sub>2</sub> plays an essential mediator in several biological reactions catalyzed by enzymes (1, 2). The excess of H<sub>2</sub>O<sub>2</sub> may potentially damage carbohydrates, lipids, and proteins in the human body (3). Thus, it is crucial to design an efficient platform for H<sub>2</sub>O<sub>2</sub> measurement in biological samples. So far, different determination schemes have been used for H<sub>2</sub>O<sub>2</sub> monitoring, such as chromatography (4), spectrophotometry (5), chemiluminescence (6), and electrochemistry (7).

Enzyme-less H<sub>2</sub>O<sub>2</sub> electrochemical sensors have the advantage of simplicity, inexpensive, high sensitivity, rapid response and suitability for real-time detection (8, 9). From this point of view, the construction of new and effective electrochemical assays for H<sub>2</sub>O<sub>2</sub> detection, especially in biological samples, has received extensive attention in re-

cent years (10, 11).

## 2. Objectives

In this work, MnO<sub>2</sub> nanoflakes were deposited on the surface fibrous structure of sepiolite clay via a facile hydrothermal process. The prepared nanocomposite (MnO<sub>2</sub>/sepiolite) was employed for the modification of a simple and low-cost carbon paste electrode (CPE). The electrocatalytic activity of the modified CPE toward H<sub>2</sub>O<sub>2</sub> was explored. The linear detection range and detection limit of the MnO<sub>2</sub>/sepiolite-CPE were also investigated in detail. Furthermore, the fabricated non-enzymatic H<sub>2</sub>O<sub>2</sub> electrochemical sensor was used for the determination of H<sub>2</sub>O<sub>2</sub> in human serum samples.

### 3. Methods

#### 3.1. Reagents and Instrument

Flake graphite (100 mesh, 99.5% purity), paraffin oil,  $\text{H}_2\text{O}_2$  (30 wt%), ammonium persulfate  $((\text{NH}_4)_2\text{S}_2\text{O}_8, 99.0\text{ purity})$ , potassium permanganate  $(\text{KMnO}_4, 99.5\text{ purity})$ , disodium hydrogen phosphate dodecahydrate  $(\text{Na}_2\text{HPO}_4 \cdot 12\text{H}_2\text{O}, 99\text{ purity})$ , and sodium dihydrogen phosphate dehydrate  $(\text{NaH}_2\text{PO}_4 \cdot 2\text{H}_2\text{O}, 99\text{ purity})$  were acquired from Merck Co. (Darmstadt, Germany). Sepiolite powder was provided by Dorkav Minig Co., Ltd. (Mashhad, Iran). Raw sepiolite was purified according to a previously reported method (12). Ultrapure water was used for the preparation of phosphate buffer solution.

Electrochemical experiments were conducted on a OriGaState100 electrochemical workstation (OriGaLys, France) using a standard electrochemical cell, including the modified CPE as the working electrode, the platinum wire as the counter electrode, and saturated calomel electrode (SCE) as the reference electrode.

#### 3.2. Synthesis of $\text{MnO}_2$ /Sepiolite Nanocomposite

$\text{MnO}_2$ /sepiolite nanocomposite was prepared via the one-step hydrothermal method, described in an earlier report (13). Briefly, 2.0 g of the purified sepiolite powder was dispersed into a 30-mL mixed solution of  $(\text{NH}_4)_2\text{S}_2\text{O}_8$  (2.21 g) and  $\text{KMnO}_4$  (1.85 g). This mixture was poured into a 50-mL Teflon-lined stainless steel autoclave and then kept in an oven at  $110^\circ\text{C}$  for 14 h. The achieved  $\text{MnO}_2$ /sepiolite material was collected and then washed repeatedly with ultrapure water. The product was further dried in an oven at  $60^\circ\text{C}$ .

#### 3.3. Electrode Fabrication

The working CPE electrode was prepared according to the methods reported previously (14, 15). Typically, materials, including flake graphite, paraffin oil, and  $\text{MnO}_2$ /sepiolite in the ratio of 67:25:8 (w/w), were mixed in a mortar for 10 min to get a homogenized carbon paste. The obtained paste was filled carefully into a Teflon tube (3 mm inner diameter and a height of 10 cm) as the body of the electrode. A copper wire was used as the electrical conductor. A fresh CPE surface was provided with polishing the electrode surface on a weighing paper.

### 4. Results

X-ray diffraction patterns of the sepiolite and  $\text{MnO}_2$ /sepiolite samples are shown in Figure 1A and B. The diffraction peaks appeared at  $2\theta = 7.7^\circ, 19.6^\circ, 20.7^\circ,$

$26.5^\circ$ , and  $34.8^\circ$  matched well with the diffraction peaks of (110), (060), (131), (080), and (441) crystal planes of sepiolite clay standard data (JCPDS card PDF file No. 13-0595) (16, 17). Two characteristic diffraction peaks at  $37.2^\circ$  and  $66.3^\circ$  could also be assigned to the (131), and (421) planes of  $\gamma\text{-MnO}_2$  (JCPDS 72-1982), respectively (18).

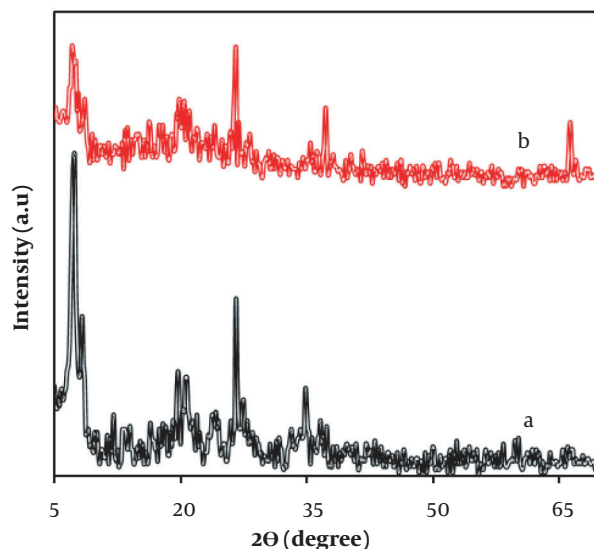


**Figure 1.** X-ray diffraction patterns of A, sepiolite; and B,  $\text{MnO}_2$ /sepiolite nanocomposite.

The TEM images of the natural sepiolite and  $\text{MnO}_2$ /sepiolite nanocomposite are shown in Figure 2A and B. As can be seen,  $\text{MnO}_2$  nanoflakes successfully deposited on the surface of the sepiolite fibers. Moreover, the EDS spectrum of the  $\text{MnO}_2$ /sepiolite nanocomposite (Figure 3) depicts the existence of Mn, O, Si, and Mg and elements in the prepared material. All the above results confirm the synthesis of  $\text{MnO}_2$ /sepiolite nanocomposite via the hydrothermal method.

### 5. Discussion

The electrochemical performances of unmodified CPE and  $\text{MnO}_2$ /sepiolite-CPE toward  $\text{H}_2\text{O}_2$  were studied by cyclic voltammetry. As presented in Figure 4, the oxidation peak current for  $\text{MnO}_2$ /sepiolite-CPE (appeared at 0.45 V) was much larger than that of the unmodified CPE, which is ascribed to the remarkable catalytic ability of  $\text{MnO}_2$ /sepiolite material toward  $\text{H}_2\text{O}_2$  oxidation on the electrode surface.

The influence of solution pH was explored on the voltammetric peak current at the  $\text{MnO}_2$ /sepiolite-CPE. As

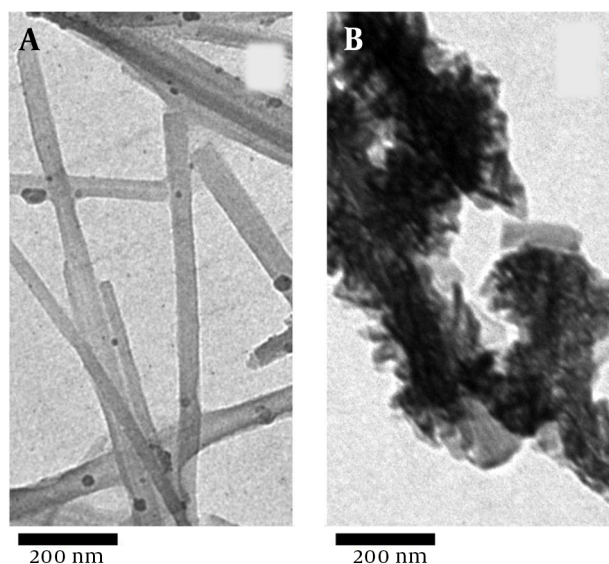


**Figure 2.** SEM images A, sepiolite; and B,  $\text{MnO}_2$ /sepiolite nanocomposite.

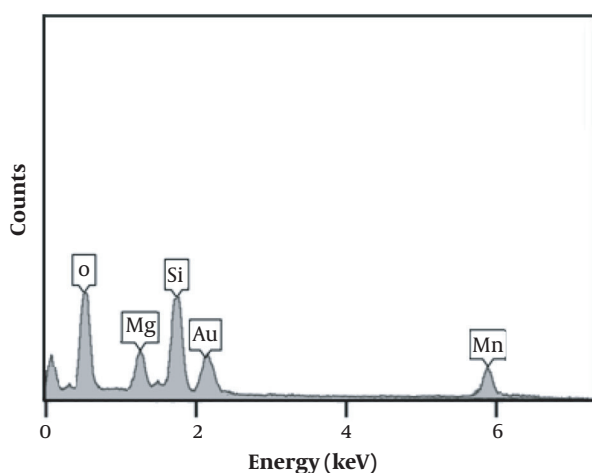


**Figure 3.** EDS spectrum of  $\text{MnO}_2$ /sepiolite nanocomposite

seen in Figure 5A, the voltammetric signals first increased with increasing pH up to 7.0, and then decreased at higher pH values. Thus, the pH 7.0 of phosphate buffer was selected for the following electrochemical tests.

The effect of  $\text{MnO}_2$ /sepiolite dose on the range of 4.0 - 12.0% (w/w) was studied by the voltammetric method in a solution containing 100  $\mu\text{M}$  of  $\text{H}_2\text{O}_2$ . As shown in Figure 5B, the maximum response can be observed at the amount of 8.0%  $\text{MnO}_2$ /sepiolite. Consequently, it was chosen as the optimal modifier amount in the next experiments.

To assess the sensitive response towards  $\text{H}_2\text{O}_2$ , the

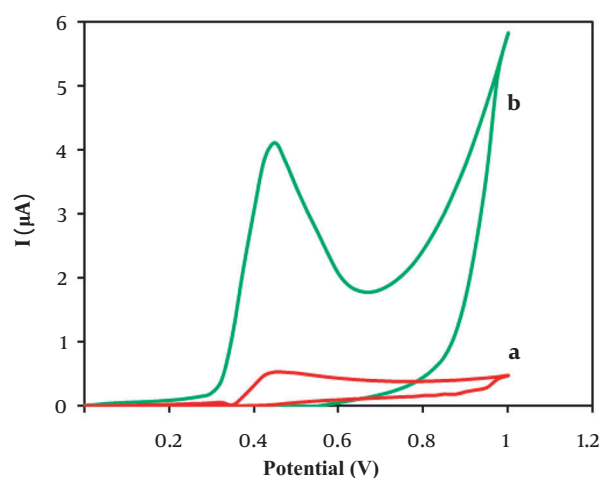


**Figure 4.** Cyclic voltammograms of the unmodified and modified electrodes in 0.1 M pH = 7 phosphate buffer at 100  $\mu\text{M}$  of  $\text{H}_2\text{O}_2$ , scan rate: 50  $\text{mV.s}^{-1}$ .

current-time (I-t) curve was explored at an applied potential of 0.5 V. The amperometric responses of the  $\text{MnO}_2$ /sepiolite-CPE with the successive injection of  $\text{H}_2\text{O}_2$  into 0.1-M buffer solution (pH 7.0) were investigated, and the results are depicted in Figure 6. The linear relationship between amperometric signal current and analyte concentration in the range of 5 - 700  $\mu\text{M}$  could be observed. Furthermore, the limit of detection (based on  $3\sigma$ ) was found to be 0.8  $\mu\text{M}$ , which was less than that of other methods (19-24) as listed in Table 1. Besides, the relative standard deviation (RSD) for ten replicate detections of 50  $\mu\text{M}$   $\text{H}_2\text{O}_2$  was calculated as 2.6%. It was also noticed that the  $\text{MnO}_2$ /sepiolite-CPE showed good stability and could be used for at least two weeks. The influence of common interfering species on the determination of 50  $\mu\text{M}$   $\text{H}_2\text{O}_2$  using the  $\text{MnO}_2$ /sepiolite-CPE was evaluated. As listed in Table 2, the 10-fold concentration of interfering molecules demonstrated nearly no interference in  $\text{H}_2\text{O}_2$  monitoring. This finding indicated the satisfactory selectivity of the suggested assay.

The practical applications of the  $\text{MnO}_2$ /sepiolite-CPE in analysis of  $\text{H}_2\text{O}_2$  in human serum samples were studied using the standard addition method. Real samples were provided from a local hospital in Tehran. The obtained results and recoveries of the spiked samples are exhibited in Table 3. These results showed that the present system is an effective platform for the monitoring of  $\text{H}_2\text{O}_2$  in real applications.

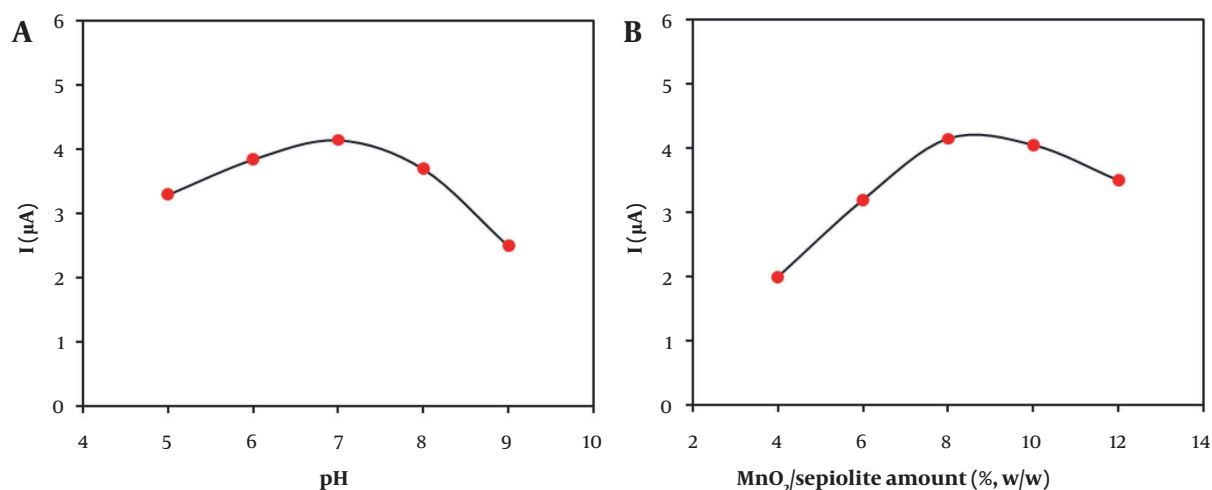


**Figure 5.** The effect of A, pH; and B, MnO<sub>2</sub>/sepiolite amount on voltammetric current response at MnO<sub>2</sub>/sepiolite-CPE in phosphate buffer (0.1 M) containing 100 μM of H<sub>2</sub>O<sub>2</sub>.

**Table 1.** Comparative Study of Various Electrochemical Sensors for H<sub>2</sub>O<sub>2</sub> Detection

Electrode Modifier*	Linear Range (μM)	Detection Limit (μM)	Ref.
MnO <sub>2</sub> nanotubes/reduced graphene oxide nanocomposite	100 - 30000	1.29	(19)
V <sub>2</sub> O <sub>5</sub> /VO <sub>2</sub> nanostructures	8 - 215	5	(20)
Cuprous oxide-reduced graphene oxide nanocomposites	30 - 12800	21.7	(21)
Poly(p-aminobenzene sulfonic acid)	50 - 550	10	(22)
Hematite nanoparticles	50 - 3145	22	(23)
Gold nanobipyramids/multi-walled carbon nanotubes	5.0 - 47300	1.5	(24)
MnO <sub>2</sub> /sepiolite nanocomposite	5 - 700	0.8	This work

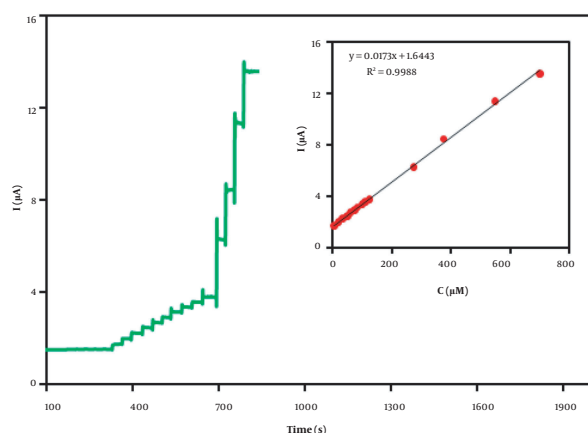


**Figure 6.** Amperometric current-time curve of MnO<sub>2</sub>/sepiolite-CPE to consecutive addition of a series of concentration (5.0 to 700.0 μM) of H<sub>2</sub>O<sub>2</sub> into 0.1 M buffer solution (pH = 7.0) at an applied potential of 0.5 V (Inset: calibration plot of sensor).

**Table 2.** Effects of Interfering Species on H<sub>2</sub>O<sub>2</sub> Detection

Foreign Molecule	Recovery (%)
Sucrose	97.9
Citric acid	98.0
Glucose	97.7
Ascorbic acid	97.2
Glutamic acid	98.6

### 5.1. Conclusion

In sum, a simple, selective, and sensitive electrochemical device for H<sub>2</sub>O<sub>2</sub> determination was proposed. The MnO<sub>2</sub>/sepiolite-CPE showed a good linear relationship with the concentration of H<sub>2</sub>O<sub>2</sub> up to 700 μM. Moreover, the suggested method showed notable selectivity for the measuring of H<sub>2</sub>O<sub>2</sub> in the presence of some interfering species. In addition, MnO<sub>2</sub>/sepiolite-CPE demonstrated

**Table 3.** H<sub>2</sub>O<sub>2</sub> Detection in Human Serum Samples

Sample	Spiked (μM)	Found (μM)	Recovery (%)	RSD <sup>a</sup>
Human serum (1)	10	9.8	98.0	3.5
	20	20.3	101.5	4.1
	30	29.4	102.0	3.4
Human serum (2)	10	10.3	103.0	3.5
	20	19.7	98.5	4.2
	30	28.9	96.3	4.0

<sup>a</sup> n = 3.

great potential application for H<sub>2</sub>O<sub>2</sub> monitoring in real biological samples.

### Footnotes

**Authors' Contribution:** AbduRahman Hosseinifar, collected the electrochemical data; Masoud Ghanei-Motlagh, developed the original idea and the protocol, abstracted and analyzed data, wrote the manuscript, and is a guarantor; Maryam Fayazi, analysis and interpretation of data and material support. All authors read and approved the final manuscript.

**Conflict of Interests:** The authors report no conflicts of interest in this work.

**Data Reproducibility:** The data presented in this study are openly available in one of the repositories or will be available on request from the corresponding author by this journal representative at any time during submission or after publication. Otherwise, all the consequences of possible withdrawal or future retraction will be with the corresponding author.

**Funding/Support:** This work is not funded by any university or company.

### References

- Heli H, Pishahang J. Cobalt oxide nanoparticles anchored to multi-walled carbon nanotubes: Synthesis and application for enhanced electrocatalytic reaction and highly sensitive nonenzymatic detection of hydrogen peroxide. *Electrochim Acta*. 2014;**123**:518–26. doi: [10.1016/j.electacta.2014.01.032](https://doi.org/10.1016/j.electacta.2014.01.032).
- Baghayeri M, Alinezhad H, Tarahomi M, Fayazi M, Ghanei-Motlagh M, Maleki B. A non-enzymatic hydrogen peroxide sensor based on dendrimer functionalized magnetic graphene oxide decorated with palladium nanoparticles. *Appl Surf Sci*. 2019;**478**:87–93. doi: [10.1016/j.apsusc.2019.01.201](https://doi.org/10.1016/j.apsusc.2019.01.201).
- Guler M, Turkoglu V, Bulut A, Zahmakiran M. Electrochemical sensing of hydrogen peroxide using Pd@Ag bimetallic nanoparticles decorated functionalized reduced graphene oxide. *Electrochim Acta*. 2018;**263**:118–26. doi: [10.1016/j.electacta.2018.01.048](https://doi.org/10.1016/j.electacta.2018.01.048).
- Gimeno P, Bousquet C, Lassu N, Maggio AF, Civade C, Brenier C, et al. High-performance liquid chromatography method for the determination of hydrogen peroxide present or released in teeth bleaching kits and hair cosmetic products. *J Pharm Biomed Anal*. 2015;**107**:386–93. doi: [10.1016/j.jpba.2015.01.018](https://doi.org/10.1016/j.jpba.2015.01.018). [PubMed: [25656490](https://pubmed.ncbi.nlm.nih.gov/25656490/)].
- Cai H, Liu X, Zou J, Xiao J, Yuan B, Li F, et al. Multi-wavelength spectrophotometric determination of hydrogen peroxide in water with peroxidase-catalyzed oxidation of ABTS. *Chemosphere*. 2018;**193**:833–9. doi: [10.1016/j.chemosphere.2017.11.091](https://doi.org/10.1016/j.chemosphere.2017.11.091). [PubMed: [29874756](https://pubmed.ncbi.nlm.nih.gov/29874756/)].
- Sheng Y, Yang H, Wang Y, Han L, Zhao Y, Fan A. Silver nanoclusters-catalyzed luminol chemiluminescence for hydrogen peroxide and uric acid detection. *Talanta*. 2017;**166**:268–74. doi: [10.1016/j.talanta.2017.01.066](https://doi.org/10.1016/j.talanta.2017.01.066). [PubMed: [28213233](https://pubmed.ncbi.nlm.nih.gov/28213233/)].
- Chen X, Cai Z, Huang Z, Oyama M, Jiang Y, Chen X. Ultrafine palladium nanoparticles grown on graphene nanosheets for enhanced electrochemical sensing of hydrogen peroxide. *Electrochim Acta*. 2013;**97**:398–403. doi: [10.1016/j.electacta.2013.02.047](https://doi.org/10.1016/j.electacta.2013.02.047).
- Ghanei-Motlagh M, Taher MA, Fayazi M, Baghayeri M, Hosseinifar A. Non-Enzymatic Amperometric Sensing of Hydrogen Peroxide Based on Vanadium Pentoxide Nanostructures. *J Electrochem Soc*. 2019;**166**(6):B367–72. doi: [10.1149/2.0521906jes](https://doi.org/10.1149/2.0521906jes).
- Ghanei-Motlagh M, Hosseinifar A. A novel amperometric hydrogen peroxide sensor based on gold nanoparticles supported on Fe<sub>3</sub>O<sub>4</sub>@polyethyleneimine. *Int J Environ Anal Chem*. 2019;**100**(5):591–601. doi: [10.1080/03067319.2019.1637859](https://doi.org/10.1080/03067319.2019.1637859).
- Chen W, Cai S, Ren QQ, Wen W, Zhao YD. Recent advances in electrochemical sensing for hydrogen peroxide: A review. *Analyst*. 2012;**137**(1):49–58. doi: [10.1039/c1an15738h](https://doi.org/10.1039/c1an15738h). [PubMed: [22081036](https://pubmed.ncbi.nlm.nih.gov/22081036/)].
- Liu H, Weng L, Yang C. A review on nanomaterial-based electrochemical sensors for H<sub>2</sub>O<sub>2</sub>, H<sub>2</sub>S and NO inside cells or released by cells. *Mikrochim Acta*. 2017;**184**(5):1267–83. doi: [10.1007/s00604-017-2179-2](https://doi.org/10.1007/s00604-017-2179-2).
- Fayazi M, Ghanei-Motlagh M. Electrochemical mineralization of methylene blue dye using electro-Fenton oxidation catalyzed by a novel sepiolite/pyrite nanocomposite. *Int J Environ Sci Technol*. 2020;**17**(11):4541–8. doi: [10.1007/s13762-020-02749-2](https://doi.org/10.1007/s13762-020-02749-2).
- Fayazi M, Afzali D, Ghanei-Motlagh R, Iraj A. Synthesis of novel sepiolite-iron oxide-manganese dioxide nanocomposite and application for lead(II) removal from aqueous solutions. *Environ Sci Pollut Res Int*. 2019;**26**(18):18893–903. doi: [10.1007/s11356-019-05119-9](https://doi.org/10.1007/s11356-019-05119-9). [PubMed: [31077042](https://pubmed.ncbi.nlm.nih.gov/31077042/)].
- Sheikh Arabi M, Karami C, Ghanei-Motlagh M. Fabrication of a Novel Electrochemical Sensor for Simultaneous Determination of Toxic Lead and Cadmium Ions. *Ann Mil Health Sci Res*. 2019;**17**(4). doi: [10.5812/amh.99082](https://doi.org/10.5812/amh.99082).
- Ghanei-Motlagh M, Taher MA. A novel electrochemical sensor based on silver/halloysite nanotube/molybdenum disulfide nanocomposite for efficient nitrite sensing. *Biosens Bioelectron*. 2018;**109**:279–85. doi: [10.1016/j.bios.2018.02.057](https://doi.org/10.1016/j.bios.2018.02.057). [PubMed: [29573727](https://pubmed.ncbi.nlm.nih.gov/29573727/)].
- Fayazi M, Ghanbarian M. One-Pot Hydrothermal Synthesis of Polyethyleneimine Functionalized Magnetic Clay for Efficient Removal of Noxious Cr(VI) from Aqueous Solutions. *Silicon*. 2019;**12**(1):125–34. doi: [10.1007/s12633-019-00105-9](https://doi.org/10.1007/s12633-019-00105-9).

17. Fayazi M, Afzali D, Taher MA, Mostafavi A, Gupta VK. Removal of Safranin dye from aqueous solution using magnetic mesoporous clay: Optimization study. *J Mol Liq*. 2015;**212**:675–85. doi: [10.1016/j.molliq.2015.09.045](https://doi.org/10.1016/j.molliq.2015.09.045).
18. He J, Wang M, Wang W, Miao R, Zhong W, Chen SY, et al. Hierarchical Mesoporous NiO/MnO<sub>2</sub>@PANI Core-Shell Microspheres, Highly Efficient and Stable Bifunctional Electrocatalysts for Oxygen Evolution and Reduction Reactions. *ACS Appl Mater Interfaces*. 2017;**9**(49):42676–87. doi: [10.1021/acsami.7b07383](https://doi.org/10.1021/acsami.7b07383). [PubMed: [29161503](https://pubmed.ncbi.nlm.nih.gov/29161503/)].
19. Mahmoudian MR, Alias Y, Basirun WJ, Woi PM, Sookhakian M. Facile preparation of MnO<sub>2</sub> nanotubes/reduced graphene oxide nanocomposite for electrochemical sensing of hydrogen peroxide. *Sens Actuators B Chem*. 2014;**201**:526–34. doi: [10.1016/j.snb.2014.05.030](https://doi.org/10.1016/j.snb.2014.05.030).
20. Fayazi M. Determination of H<sub>2</sub>O<sub>2</sub> in Human Serum Samples with Novel Electrochemical Sensor Based on V<sub>2</sub>O<sub>5</sub>/VO<sub>2</sub> Nanostructures. *Ann Mil Health Sci Res*. 2019;**17**(3). doi: [10.5812/amh.96175](https://doi.org/10.5812/amh.96175).
21. Xu F, Deng M, Li G, Chen S, Wang L. Electrochemical behavior of cuprous oxide-reduced graphene oxide nanocomposites and their application in nonenzymatic hydrogen peroxide sensing. *Electrochim Acta*. 2013;**88**:59–65. doi: [10.1016/j.electacta.2012.10.070](https://doi.org/10.1016/j.electacta.2012.10.070).
22. Kumar S, Chen S. Electrocatalytic reduction of oxygen and hydrogen peroxide at poly(p-aminobenzene sulfonic acid)-modified glassy carbon electrodes. *J Mol Catal A Chem*. 2007;**278**(1-2):244–50. doi: [10.1016/j.molcata.2007.09.023](https://doi.org/10.1016/j.molcata.2007.09.023).
23. Cai J, Ding S, Chen G, Sun Y, Xie Q. In situ electrodeposition of mesoporous aligned  $\alpha$ -Fe<sub>2</sub>O<sub>3</sub> nanoflakes for highly sensitive nonenzymatic H<sub>2</sub>O<sub>2</sub> sensor. *Appl Surf Sci*. 2018;**456**:302–6. doi: [10.1016/j.apsusc.2018.06.108](https://doi.org/10.1016/j.apsusc.2018.06.108).
24. Mei H, Wang X, Zeng T, Huang L, Wang Q, Ru D, et al. A nanocomposite consisting of gold nanobipyramids and multiwalled carbon nanotubes for amperometric nonenzymatic sensing of glucose and hydrogen peroxide. *Mikrochim Acta*. 2019;**186**(4):235. doi: [10.1007/s00604-019-3272-5](https://doi.org/10.1007/s00604-019-3272-5). [PubMed: [30868243](https://pubmed.ncbi.nlm.nih.gov/30868243/)].